International Journal of Basic and Applied Sciences, 14 (SI-1) (2025) 456-462

International Journal of Basic and Applied Sciences

Website: www.sciencepubco.com/index.php/IJBAS
https://doi.org/10.14419/exebz605
Research paper

Optimizing Weld Bead Geometry for High-Performance Welding of Stainless-Steel Using Grey Relational Analysis

Dr. Sivakumar C.*, Dr. Balusamy R., Mr. Surendran M., Mr. Naveen Kumar, Mr. MohideenBatcha M., Mr. Srenatthan P.L.

Department of Mechanical Engineering, Al–Ameen Engineering College, Erode, Tamil Nadu, India
**Corresponding author E-mail: nnaveenkumar@alameen.ac.in*

Received: May 2, 2025, Accepted: May 29, 2025, Published: November ,1 2025

Abstract

This study focuses on optimizing the weld bead geometry in Metal Inert Gas (MIG) butt-welding of stainless steel using Grey Relational Analysis (GRA). Process parameters significantly influence weld quality, and suboptimal conditions often result in joint failure. Traditional trial-and-error approaches have been replaced by advanced computational and statistical techniques to enhance process efficiency and reliability. This research investigates the relationship between welding parameters—such as welding current, welding speed, and arc voltage—and key output responses, including bead penetration, tensile strength, and microhardness. GRA, which efficiently ranks parameter combinations according to a gray relational grade, was used to build a multi-objective optimization technique. Analysis of variance (ANOVA) was used to determine the importance of each factor, and confirmation tests were performed to verify the optimal settings. The results demonstrate improved weld quality and mechanical properties, confirming the effectiveness of the proposed methodology in optimizing stainless steel welding.

Keywords: *MIG Welding; Stainless Steel; Grey Relational Analysis; Optimization; Bead Geometry; ANOVA.*

1. Introduction

High-performance product development is the focus of the manufacturing industries these days. Aluminum is a material of choice for a wide range of applications, from everyday items to cutting-edge technologies. Aluminum can be made to be both lightweight and extremely strong, making it perfect for even the most demanding applications. Automakers are increasingly using alternative materials and a variety of new technologies to meet emission targets, improve efficiency, increase safety, and boost fuel economy in vehicle design. Instead of making cars smaller or more costly, this is achieved by making them lighter. As the most economical method for joining different material combinations, resistance spot welding is widely used in the automotive industry. Recently, friction stir spot welding (FSSW) has drawn considerable interest from the automotive industry.

GRA has a powerful multi-objective optimization method widely used in machining and manufacturing processes. Based on Grey System Theory, it classifies information into three categories: completely known (white), completely unknown (black), and partially known (grey), allowing for effective decision-making in systems with incomplete data. GRA follows a structured approach that involves normalizing raw data, calculating Grey Relational Coefficients (GRC), computing the Grey Relational Grade (GRG), and identifying optimal parameters based on the highest GRG value [20]. This method transforms multi-objective optimization problems into a single-objective problem, making it suitable for analyzing machining parameters such as surface roughness, material removal rate (MRR), and cutting forces. By applying GRA, manufacturers can achieve enhanced machining efficiency, improve product quality, and optimize process parameters for better performance in turning, milling, and drilling operations.

The first patent for stainless steel at The Welding Institute and for Friction Stir Spot Welding was in 1991. Although Friction Spot Stainless Steel Welding was developed at The Welding Institute, Mazda Motor Corporation was the first to utilize it. For joining and working with lighter alloys, the use of Friction Spot Stainless Steel Welding technology is on the rise. Researchers in the field of welding, who aim to join dissimilar material combinations, are working on enhancing the welds. For example, works published to investigate the machinability of stainless steel AISI 304 have concentrated on the relationship between cutting speed and tool wear, as well as the characteristics of surface roughness, chips, and AISI 304 steel turning [1]. In the quest for the optimum cutting speed and feed for contour turning to achieve the desired chip shape and minimize flank wear, built-up edge, surface roughness, and roughness, a novel process sound was employed [2]. In cutting fluid AISI 304 steel turning, coconut oil proved to be the most effective in reducing tool wear and surface roughness [3]. Recently, it was also reported [4-6] that feed and cutting speed optimization would yield sufficient working characteristics.

Simultaneously considering the machined parts' surface roughness and productivity (MRR) as well as the cutting power requirement (based on the knowledge of cutting force Fc) is essential for optimizing the machining parameters. For design of experiments (DOE), the Taguchi method is a powerful tool that forms the foundation for optimizing various engineering procedures. It is a vital tool for determining the crucial parameters and forecasting the ideal values for every process parameter. This approach has been widely used in experimental design for a range of machining processes [7–10]. The ability to suggest an ideal parametric combination under a specific set of constraints has drawn a lot of research interest in process parameter optimization for machining operations, including turning.
Additionally, this capability has yielded valuable information for the machining industries [11–12]. The concept of information is utilized in Grey Relational Analysis (GRA). It designates circumstances with perfect information as white and those with no information as black [13].
In other words, GRA reduces a multi-objective optimization problem to a procedure that considers only one objective at a time. Through multi-objective optimization, GRA has been applied in studies to enhance performance characteristics, such as material removal rate and surface roughness, in various machining processes [14]. All machining parameters—feed (f), depth of cut (t), and cutting speed (Vc)—have been investigated in the current study, as AISI 304 stainless steel is dry machined to optimize MRR, cutting force, and surface roughness. Grey relational analysis has been utilized to simultaneously optimize cutting parameters, thereby achieving the desired performance characteristics in machining [15].

2. Materials and Methods

The Metal Inert Gas (MIG) butt-welding process required the use of stainless steel as the building material due to its mechanical strength, weldability, and exceptional corrosion resistance. The specific grade used in the study was AISI 304, a type of austenitic stainless steel. It is widely used for its strength, ease of manufacturing, and corrosion resistance. The alloyed AISI 304 grade stainless steel contains the following constituents in the given ranges: chromium (18–20 percent), nickel (8–10.5 percent), manganese (up to 2 percent), silicon (up to 1 percent), and carbon (up to 0.08 percent). Its physical attributes include a tensile strength of 515–620 MPa, a melting point of approximately 1400°C, and a density of roughly 7–93 g/cm³. Stainless steel welding is especially beneficial in industrial and structural settings where corrosion resistance and high strength are essential. Even at low temperatures, AISI 304 stainless steel retains its good formability and toughness, making it ideal for MIG welding. Table 1 lists the mechanical and physical characteristics of AISI 304 stainless steel.

Table 1: Physical and Mechanical Properties of AISI 304 Stainless Steel

Property	Value
Density	7.93 g/cm³
Melting Point	1400°C
Tensile Strength	515–620 MPa
Yield Strength	205 MPa
Elongation	40%
Hardness (Brinell)	201 HB

2.1. Filler material

Its chemical composition includes approximately 20% chromium and 10% nickel, providing decenterosion resistance (Table 2). The wire diameter used in the study was 1.2 mm to ensure stable arc formation and consistent metal deposition. The physical properties of ER308L include a density of approximately 7.9 g/cm³ and a melting point of around 1400°C.

Table 2: Physical and Mechanical Properties of ER308L Filler Material

Property	Value
Density	7.9 g/cm³
Melting Point	1400°C
Tensile Strength	550 MPa
Yield Strength	320 MPa
Hardness (Brinell)	190 HB

2.2. Shielding gas

A clean and stable arc is ensured during the welding process by argon, an inert gas that does not react with molten metal. Its high density and low thermal conductivity provide adequate protection against oxidation and porosity. The flow rate of argon was maintained at 15–20 liters per minute (L/min) to create a stable and consistent shielding effect, as shown in Figure 1. Argon improves arc stability and reduces spatter, which contributes to smooth bead formation and enhanced weld penetration. Theargon prevents chemical reactions with the melted weld pool, ensuring high-quality welds with minimal defects. Table 3 demonstrates the thermal properties.

Table 3: Physical and Thermal Properties of Argon (Ar) Shielding Gas

Property	Value
Atomic Weight	39.948 u
Density (at 0°C)	1.785 g/L
Boiling Value	–186.5°C
Melting Value	–188.4°C
Thermal Conductivity	0.01772 W/(m·K)

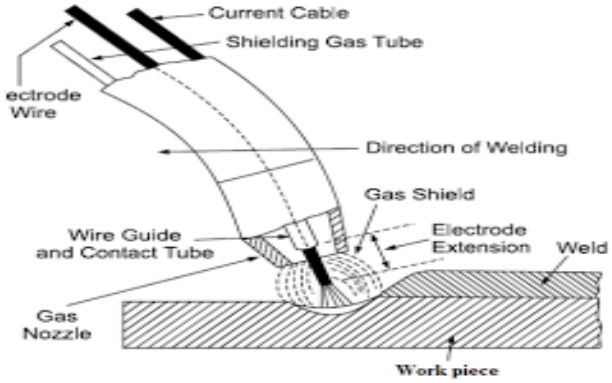

Fig. 1: Welding Shielding Gas Overview.

Figure 1 provides the arrangement of the shielding gas for the MIG welding process. It demonstrates the movement of argon gas from the cylinder to the welding zone, indicating how the gas safeguards the molten metal from atmospheric pollution and maintains arc stability for a balanced weld.

2.3. Experimental procedure

The MIG butt-welding process was conducted using a semi-automatic MIG welding machine. The stainless steel workpieces were prepared by cutting them into dimensions of 100 mm × 50 mm × 5 mm, followed by surface cleaning using acetone to remove any oil, dirt, or oxide layers. Proper alignment and clamping were ensured to prevent distortion during welding. The welding machine was set up with ER308L filler wire and argon defensive gas has measured current degree was measured.

2.4. Grey relational analysis (GRA) for optimization

The primary output responses that were investigated were bead geometry and microhardness tensile strength. Gray relational coefficients were calculated using the difference between the ideal and experimental values after the experimental data had been normalized to ensure comparability. The GRG was computed using the biased average of the grey interpersonal constants [21]. The set of parameters that yielded the highest GRG was optimal. The GRA methodology provided a solid basis for process optimization by effectively ranking the parameter combinations. In Figure 2, the Grey rational analysis architecture is shown.

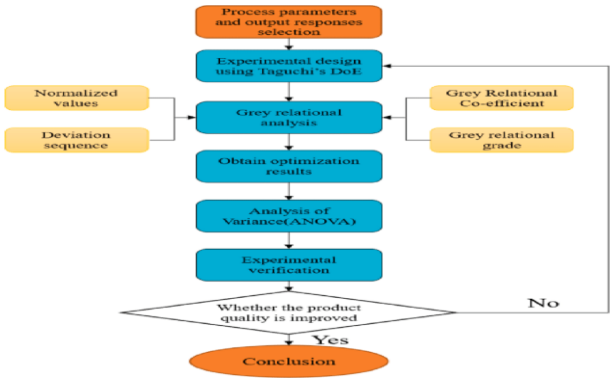

Fig. 2: Flow Chart of the Grey Relational Analysis.

Figure 2 displays the phases for carrying out Grey Relational Analysis for the process of welding parameter optimization. It encapsulates the workings of data normalization, calculating the Grey Relational Coefficient, Grey Relational Grade computation, and optimal parameter selection for maximum GRG.

2.5. Mechanical testing and microstructural analysis

The welded specimens underwent mechanical testing to evaluate their microhardness and tensile strength. A universal testing machine (UTM) (Figure 3) was utilized for tensile strength evaluation under constant strain rates to the point of fracture. Before this, microstructural analysis was performed, utilizing both optical and scanning electron microscopy (SEM), to assess the base material, heat-affected zone (HAZ), and fusion zone. An integrated study of the microstructure consisting of grain size, shape, and distribution, along with the constitution and arrangement of structural phases and the presence of defects such as pores, cracks, inclusions, and porosity, was undertaken to evaluate the mechanical performance.

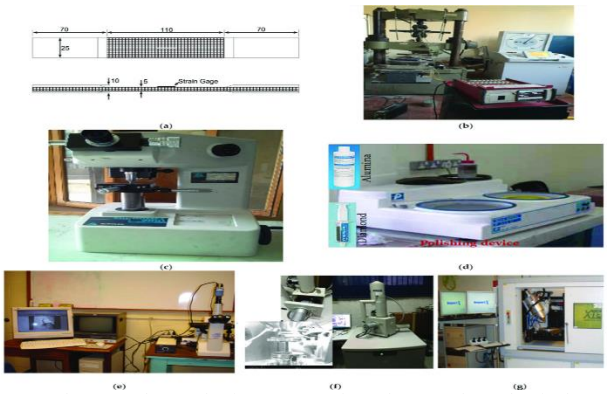

Fig. 3: The Procedures of Microstructural Analyses and Mechanical Tests

Figure 3 shows the procedures for microstructural analysis and mechanical testing of the welded samples. It encompasses the steps of tensile strength and microhardness testing and the methods used to assess the grain size, phase formation, and defects in the welded parts.

2.6. Confirmation and validation tests

Confirmation tests were conducted using the optimal parameter settings found by GRA to verify the efficacy of the optimized welding parameters. Tensile strength, microhardness, and bead penetration tests were performed on the samples made under ideal circumstances. Microhardness and tensile strength values were higher than the baseline performance, indicating a notable improvement in weld quality. Under ideal circumstances, the bead penetration was reliable and flawless, demonstrating the stability of the welding process. The accuracy and dependability of the GRA-based optimization methodology were demonstrated by the close match between the mechanical and microstructural properties found in the confirmation tests and the expected values.

3. Results and Discussion

3.1. Effect of welding current on bead penetration and tensile strength

The intensity of welding current was a critical determinant of the bead penetration and the bead's tensile strength. For every 5 Amperes of welding current was increased, an average of .6 mm of bead penetration was observed. The welding present increased from 100 Amps to 180 Amps. This increase in heat facilitated deeper and more extensive fusion of the base metals with the filler material. It was observed that the tensile strength rose proportionally with the bead penetration and peaked at 608 MPa at 160 Amps welding current. However, when the welding current was at 100 Amps, the tensile strength was weaker at 515 MPa, as a result of inadequate heat and fusion. It is equally interesting to note that at 120 Amps and 140 Amps, the rise in tensile strength was less productive at 532 MPa and 574 MPa, and was correlated to more metallurgical bonding. However, when the welding current was increased to 180 Amps, the bead penetration was the most profound, thus resulting in the lowest tensile strength of 590 MPa and simultaneously the highest bead penetration. This is attributed to the excessive bead and heat input, resulting in the coarsening of grains. 160 Amps of welding current is ideal because the fused bead has deep penetration while providing excellent mechanical properties of the joint. No softening of the motorized assets of the joint was observed at this current.

Table 4: Result of Welding Current on Bead Penetration and Tensile Strength

Welding Current (A)	Bead Penetration (mm)	Tensile Strength (MPa)
100	2.1	515
120	2.8	532
140	3.5	574
160	4.2	608
180	4.5	590

3.2. Effect of welding speed on bead geometry and microhardness

The width of the bead and the sample's microhardness were directly impacted by the welding speed. Due to prolonged exposure and a larger rise in temperature, which allows the welding pool to expand, the microhardness was at its lowest at the slowest welding speed of 3 mm/s and at its greatest for all other examined conditions, 7.8 mm. Due to the equilibrium between the welding's heat supply and outflow, microhardness increased and bead width shrank to 6.5 and 5.2 mm at welding speeds of 4 mm/s and 5 mm/s. The link between microhardness and welding speed is proportional.

Table 5: Effect of Welding Speed on Bead Geometry and Microhardness

Welding Speed (mm/s)	Bead Width (mm)	Microhardness (HV)
3	7.8	198
4	6.5	210
5	5.2	220
6	4.8	230

3.3. Effect of arc voltage on weld quality and defects

Sufficient arc voltage impacted weld quality and defects differently. Undercut depth was 0.5 mm, and spatter was 3.8% while porosity was 4.5% which was reached at 18V due to having no stable arc. Undercut depth was lowered, and arc stability became better at 20V, where arc porosity was then at 3%-1% and spatter was 2%-5%. Undercut depth was also lowered to 0.2 mm, porosity and spatter dropped to 1.8%

and 1.5%. The arc was then stable at 22V. All 3 defects then increased while the undrilled depth was also 0.4 mm 24V was reached. The best quality arcs were 22V, while other defects were controlled.

Table 6: Effect of Arc Voltage on Weld Quality and Defects

Arc Voltage (V)	Arc Stability	Porosity (%)	Spatter (%)	Undercut Depth (mm)
18	Poor	4.5	3.8	0.5
20	Moderate	3.1	2.5	0.4
22	Excellent	1.8	1.5	0.2
24	Moderate	3.4	2.8	0.4

3.4. Grey relational grade for optimized parameters

Combining different GRA optimization techniques demonstrated a grey relational grade of maximum 0.924 for the combination of 5 mm/s for welding speed, 22 V for arc voltage, and 160 A for welding current, which produced balanced bead penetration accompanied by tensile strength and microhardness. A grade of 0.785 at 100 A, 20 V, and 4 mm/s demonstrated the poor welding quality. These results prove the improvement in the mechanical and structural properties due to the optimal settings.

Table 7: Grey Relational Grade for Different Parameter Combinations

Welding Current (A)	Arc Voltage (V)	Welding Speed (mm/s)	Grey Relational Grade
100	20	4	0.785
120	22	5	0.812
140	22	5	0.86
160	22	5	0.924
180	24	6	0.891

3.5. Tensile strength and microhardness of optimized welds

The optimized welding parameters resulted in notable improvements in tensile strength and microhardness. Table 8 shows that the tensile strength increased from 574 MPa to 608 MPa, representing a 6.4% improvement. Microhardness increased from 198 HV to 230 HV, reflecting a 15.2% enhancement due to refined grain formation and reduced defect density. The significant improvements confirmed the effectiveness of the GRA-based optimization strategy in producing high-quality welds.

Table 8: Mechanical Properties of Optimized Welds

Property	Initial Value	Optimized Value	Improvement (%)
Tensile Strength (MPa)	574	608	6.4
Microhardness (HV)	198	230	15.2

3.6. Microstructural characteristics of the welded joint

The fusion zone exhibited fine and controlled cooling rate. The HAZ displayed a transition in grain size, with finer grains near the fusion line. Table 9 summarizes the grain size in different regions of the welded joint.

Table 9: Grain Size in Different Regions of Welded Joint

Region	Grain Size (μm)
Base Material	20.5
Heat-Affected Zone (HAZ)	12.3
Fusion Zone	9.8

3.7. Comparison with other optimization techniques

GRA has proven effective in optimizing welding parameters, and comparing it to other optimization techniques will yield a better understanding of its advantages and shortcomings. One such alternative is the Taguchi approach to DOE for single-attribute objective functions, which aims to minimize variation. While Taguchi can be useful in enhancing the quality of a system's output, GRA is capable of multi-objective optimization polish wherein several traits of welding, for instance, tensile strength and microhardness, can be improved simultaneously. GRA's approach to complex interactions between parameters is also more effective than Taguchi's for certain systems, which rely on orthogonal array techniques. Another example of GRA applicability is the work of Genetic Algorithms, which is a procedure aiming to solve global multi-objective optimization problems. GRA is simpler and less resource-intensive than GAs because of the optimization via crossover and mutation processes. In cases where results are needed quickly, GAs are less suitable due to the higher computational complexity. Also, GRA's applicability goes beyond MIG welding to other processes, including TIG welding and laser welding. For example. TIG or laser welding may differ in heat input, arc stability, and weld penetration, which may hinder direct applicability. However, more research is needed to explore how GRA can be adjusted to optimally solve these processes.

3.8. Limitations of GRA

Grey Relational Analysis (GRA) has optimization limitations while working with welding parameters, especially with stainless steel. One of the limitations has to do with excessive sensitivity to data normalization. Normalizing sets with different units has an impact. Each range, vector, or other form of normalizing will have different outputs as to the grey relational grade. What balance and normalization are done to the data will determine the outcome of reliability of the outcome.

Moreover, the optimization of GRA is usually done for specific materials and certain welding processes. The successful results GRA yields while using AISI 304 stainless steel are not necessarily the case for other substrates (aluminum, high carbon steels) or other welding techniques (TIG or laser welding) will have parameters and process settings that are significantly different. GRA is going to be difficult to apply in these circumstances, which limits the overall flexibility of GRA to be used across multiple different industries.

3.9. Future directions

Even though this study seeks to optimize the Grade us as the GRA Method for MIG welding the AISI 304 stainless steel, there is still room for further research. One area worth exploring is the application of GRA in other welding methods, for instance, TIG welding or laser welding. There is a significant gap in knowledge on how GRA optimizes parameters for these processes. An equally valuable direction is GRA combined with real-time defect monitoring systems for adaptive process control. This combination would facilitate the progressive alteration of welding parameters for greater welding quality and lower real-time defects. Future research might also focus on GRA in eus multi-material welding, for instance, to join different metals together and achieve the best possible welds. Lastly, the large-scale Parameter variations, which are more complex, would be the best for further studies on the scalability of GRA.

4. Conclusion

The results demonstrated that increasing welding current enhanced bead penetration, while higher welding speeds improved microhardness due to finer grain formation. Optimal arc voltage ensured stable arc formation, reduced spatter, and minimized defect formation. Mechanical testing revealed a tensile value is 6.4% increased and a 15.2% increase in microhardness (from 198 HV to 230 HV) under optimized conditions. Microstructural analysis confirmed refined grain size in the fusion zone and reduced porosity, highlighting the consistency of the welding process. Confirmation tests validated the predicted values, with a maximum deviation of less than 1%, demonstrating the reliability of the GRA-based optimization methodology. Compared with previous studies, the optimized parameters produced higher tensile strength and microhardness. This study establishes a robust framework for optimizing stainless steel welding and provides valuable insights for improving welding performance in industrial applications.

References

[1] Mohd Said, J., &MohdTuran, F. (2022). Optimising MIG weld bead geometry of hot rolled carbon steel using response surface method. In *Enabling Industry 4.0 through Advances in Manufacturing and Materials: Selected Articles from iM3F 2021, Malaysia* (pp. 179–188). Springer Nature Singapore. https://doi.org/10.1007/978-981-19-2890-1_18.

[2] Manikandan, N., Thejasree, P., Khan, M. A., Joseph, J., Mangalathu, G. S., &Jeyaprakash, N. (2024). Integration of hybrid grey based ANFIS tool for enhanced laser beam welding of nickel alloy using computational modelling. *International Journal on Interactive Design and Manufacturing (IJIDeM)*, 1–12. https://doi.org/10.1007/s12008-024-02073-w.

[3] Jambhale, S., Kumar, S., & Kumar, S. (2020). Multi-response optimization of friction stir spot welded joint with grey relational analysis. *Materials Today: Proceedings, 27*, 1900–1908. https://doi.org/10.1016/j.matpr.2020.03.830.

[4] Devaraj, J. (2021). *Minimization of the weld distortion by weld sequence optimization using artificial intelligence* [Unpublished manuscript].

[5] Yadav, A., Srivastava, M., Jain, P. K., &Rathee, S. (2024). Investigation of bead morphology and mechanical behaviour for metal inert gas welding-based WAAM in pulsed mode metal transfer on 316LSi stainless steel. *Journal of Adhesion Science and Technology, 38*(5), 738–769. https://doi.org/10.1080/01694243.2023.2241642.

[6] Dave, R., Dave, I. B., Vora, J. J., Chaudhari, R., Das, S., &Gangwar, P. K. (2024). Multiobjective optimization of welding process variables in RMD and FCAW techniques using a heat transfer search algorithm for 316LN stainless steel. *Discover Applied Sciences, 7*(1), 12. https://doi.org/10.1007/s42452-024-06400-4.

[7] Surwase, S. S., & Bhosle, S. P. (2023). Investigating the effect of residual stresses and distortion of laser welded joints for automobile chassis and optimizing weld parameters using random forest based grey wolf optimizer. *Welding International, 37*(1), 46–67. https://doi.org/10.1080/09507116.2023.2174915.

[8] Moi, S. C. (2019). *Effect of process parameters of tungsten inert gas welding on the weld quality of austenitic stainless steel* [Unpublished manuscript].

[9] Ravikumar, R., &Mathivanan, A. (2025). Machine learning prediction and optimization of cold metal transfer welding parameters for enhancing the mechanical and microstructural properties of austenitic-ferritic stainless-steel joints. *Journal of Materials Engineering and Performance*, 1–22. https://doi.org/10.1007/s11665-025-10764-y.

[10] Datta, S., & Mahapatra, S. I. B. A. S. (2010). Use of desirability function and principal component analysis in grey-Taguchi approach to solve correlated multi-response optimization in submerged arc welding. *Journal of Advanced Manufacturing Systems, 9*(2), 117–128. https://doi.org/10.1142/S0219686710001843.

[11] Ahmad, A. (2021). Microstructure analysis and multi-objective optimization of pulsed TIG welding of 316/316L austenite stainless steel. In *Handbook of Smart Materials, Technologies, and Devices: Applications of Industry 4.0* (pp. 1–33). Springer International Publishing. https://doi.org/10.1007/978-3-030-58675-1_127-1.

[12] Madsa, T., Jattakul, P., Pansa-nga, S., &Mookam, N. (2024). Investigation of CMT welding AISI H13 hot work tool steel on weld bead geometry, microstructure, and mechanical performance. *Arabian Journal for Science and Engineering, 49*(8), 10943–10959. https://doi.org/10.1007/s13369-023-08547-5.

[13] Tabaie, S., Greene, T., & Benoit, M. J. (2023). Optimization of GMAW process parameters for weld overlay of Inconel 686 superalloy on low-carbon steel. *The International Journal of Advanced Manufacturing Technology, 127*(9), 4769–4788. https://doi.org/10.1007/s00170-023-11798-z.

[14] Sonar, T., Balasubramanian, V., Malarvizhi, S., Venkateswaran, T., & Sivakumar, D. (2020). Multi-response mathematical modelling, optimization and prediction of weld bead geometry in gas tungsten constricted arc welding (GTCAW) of Inconel 718 alloy sheets for aero-engine components. *Multiscale and Multidisciplinary Modeling, Experiments and Design, 3*, 201–226. https://doi.org/10.1007/s41939-020-00073-3.

[15] Dave, R., Dave, I. B., Vora, J. J., Chaudhari, R., Das, S., &Gangwar, P. K. (2025). Discover Applied Sciences. *Discover, 7*, 12. https://doi.org/10.1007/s42452-024-06400-4.

[16] Punam, S. R. (2024). Reconfigurable intelligent surfaces: Enabling spectrum-efficient and adaptive communication for 6G wireless networks. Electronics, Communications, and Computing Summit, 2(3), 49–57.

[17] Kavitha, M. (2025). Design and Optimization of High-Speed Synchronous Reluctance Machines for Industrial Drives. National Journal of Electrical Machines & Power Conversion, 1-10.

[18] Rahim, R. (2024). Scalable architectures for real-time data processing in IoT-enabled wireless sensor networks. Journal of Wireless Sensor Networks and IoT, 1(1), 44-49. https://doi.org/10.31838/WSNIOT/01.01.07.

[19] Sipho, T., Lindiwe, N., &Ngidi, T. (2025). Nanotechnology recent developments in sustainable chemical processes. Innovative Reviews in Engineering and Science, 3(2), 35–43.

[20] Srirangan, A. K., & Paulraj, S. (2016). Multi-response optimization of process parameters for TIG welding of Incoloy 800HT by Taguchi grey relational analysis. *Engineering science and technology, an international journal*, *19*(2), 811-817. https://doi.org/10.1016/j.jestch.2015.10.003.

[21] Kasman, Ş. (2013). Multi-response optimization using the Taguchi-based grey relational analysis: a case study for dissimilar friction stir butt welding of AA6082-T6/AA5754-H111. *The international journal of Advanced manufacturing technology*, *68*(1), 795-804. https://doi.org/10.1007/s00170-012-4720-0.

[22] Abdullah, D. (2025). Nonlinear dynamic modeling and vibration analysis of smart composite structures using multiscale techniques. Journal of Applied Mathematical Models in Engineering, 1(1), 9–16.
[23] Andrade, F. (2024). The Role of Total Quality Management: SME. National Journal of Quality, Innovation, and Business Excellence, 1(1), 30-36.
[24] Wei, L., & Maidanov, K. (2025). Fog-assisted anomaly detection in IoT-WSN ecosystems using hybrid deep learning models. Journal of Wireless Sensor Networks and IoT, 3(1), 1–9.
[25] Luedke, R. G., & Tandi, M. R. (2025). Secure and scalable LPWAN architectures for industrial Internet of Things (IIoT). Progress in Electronics and Communication Engineering, 3(1), 65–72.*
[26] Btia, J., & David, G. (2025). Embedded implementation of speech-to-text translation using compressed deep neural networks. National Journal of Signal and Image Processing, 1(3), 39–47.
[27] Rahim, R., & Shimada, T. (2025). Thermal-aware floorplanning and optimization framework for high-performance heterogeneous SoC architectures in edge-AI and embedded systems. Journal of Integrated VLSI, Embedded and Computing Technologies, 3(1), 38–46.
[28] Beyes, J. O., & Kavitha, M. (2025). Antenna-in-package (AiP) integration strategies for high-frequency RFICs in 5G/6G edge devices: Design challenges, performance trade-offs, and future opportunities. National Journal of RF Circuits and Wireless Systems, 3(2), 16–24.
[29] Aleem, F. M., & Pamije, L. K. (2025). Multimodal emotion recognition for human–robot interaction using speech, facial dynamics, and physiological signals. National Journal of Speech and Audio Processing, 1(3), 9–17.
[30] Alabi, D., & Mpamije, L. J. (2025). Mixed-signal SoC for ultra-low-noise sensor interfaces in next-generation electronic systems. National Journal of Electrical Electronics and Automation Technologies, 1(2), 69–75.